ACTA ABP BIOCHIMICA POLONICA

Vol. 63, No 1/2016
103–109
http://dx.doi.org/10.18388/abp.2015_1065

Regular paper

Crystal and molecular structure of hexagonal form of lipase B from *Candida antarctica*

Paweł Strzelczyk[1], Grzegorz D. Bujacz[1], Piotr Kiełbasiński[2] and Jarosław Błaszczyk[2]✉

[1]Lodz University of Technology, Institute of Technical Biochemistry, Łódź, Poland; [2]Centre of Molecular and Macromolecular Studies, Polish Academy of Sciences, Department of Heteroorganic Chemistry, Łódź, Poland

During crystallization screenings of commercially available hydrolytic enzymes, the new, hexagonal crystal form of CAL-B, has been discovered and hereby reported. The NAG molecules, which were closing the glycosylation site in the orthorhombic form, in hexagonal structure make the glycosylation site open. It is unknown whether the opening and closing of the glycosylation site by the 'lid' NAG molecules, could be related to the opening and closing of the active center of the enzyme upon substrate binding and product release.

Key words: CAL-B, lipase B, *Candida antarctica*, apo form, crystallographic polymorphism, macromolecular crystallography

Received: 21May, 2015; revised: 07 October, 2015; accepted: 18 November, 2015; available on-line: 30 December, 2015

INTRODUCTION

Lipases (EC 3.1.1.3) catalyze the hydrolysis of carboxylic acid esters in aqueous media but also the esterification or transesterification in organic solvents (Bornscheuer & Kazlauskas, 1999; Paravidino *et al.,* 2012; Singh *et al.,* 2012). The studies on applying commercially available hydrolytic enzymes, including lipase B from *Candida antarctica* (CAL-B), *Candida rugosa* lipase (CRL), lipase *PS Amano*, *AK Amano*, *AH Amano* or lipoprotein lipase (LPL), to the synthesis of chiral non-racemic heteroorganic compounds, have been carried out in our Department for many years (Kaczmarczyk *et al.,* 2011; Kiełbasiński *et al.,* 2003; Kiełbasiński & Mikołajczyk, 2007; Krasiński *et al.,* 2012; Kwiatkowska *et al.,* 2011; Rachwalski *et al.*, 2008). We have decided to make theoretical (Krasiński *et al.,* 2012) and experimental attempts to explain the catalytic mechanism of the enzymes and the nature of their promiscuous behavior.

There is only limited information in literature regarding the crystal structure and active site architecture of these enzymes. In the Protein Data Bank (PDB), there are 12 structures available for lipase B from *Candida antarctica* (CAL-B): 1TCA, 1TCB and 1TCC (Uppenberg *et al.,* 1994), 1LBS and 1LBT (Uppenberg *et al.,* 1995), 3ICV and 3ICW (Qian *et al.,* 2009), 4K5Q, 4K6G, 4K6H, and 4K6K (Xie *et al.,* 2014), and 3W9B (Kim *et al.,* 2014). For *Candida rugosa* lipase (CRL), there are 9 structures: 1CRL (Grochulski *et al.,* 1993), 1GZ7 (Mancheno *et al.,* 2003), 1LPM and 1LPS (Cygler *et al.,* 1994), 1LPN, 1LPO, and 1LPP (Grochulski *et al.,* 1994a), 1TRH (Grochulski *et al.,* 1994b), and 3RAR (Colton *et al.,* 2011). For lipase *PS Amano*, there is one PDB entry, 1OIL (Kim *et al.,* 1997). For lipases *AK Amano*, *AH Amano*, and lipoprotein lipase (LPL), there are no X-ray crystal structures reported to date.

All above mentioned structures are insufficient to explain the mechanism of action of these enzymes towards the heteroorganic substrates and their analogs which we use in enzyme-controlled chemical reactions conducted in our laboratory (Kaczmarczyk *et al.,* 2011; Kwiatkowska *et al.,* 2011; Krasiński *et al.,* 2012). For that reason, the crystal structures of the enzymes in the appropriate complex forms, i.e., with the particular substrates or analogs that we use, are needed. We hope that our results will shed more light not only on the catalytic mechanism of these enzymes, but also will explain the nature of the enzymes promiscuous behavior.

Among commercially available lipases, which are nowadays expressed in large quantities, lipase B from *Candida antarctica* (CAL-B) is one of the most extensively used biocatalysts, both in the research and in the industry (Kirk & Christensen, 2002; Wu *et al.,* 2013). CAL-B belongs to the α/β-hydrolase family and follows the same reaction mechanism as the other serine hydrolases (Bornscheuer & Kazlauskas, 1999; Paravidino *et al.,* 2012; Singh *et al.,* 2012). This enzyme is highly stereoselective in a wide variety of chemical transformations. A broad range of CAL-B applications includes kinetic resolution of racemic alcohols and amines or desymmetrization of diols and diacetates (Alatorre-Santamaria *et al.,* 2011; Deska *et al.,* 2010; Frykman *et al.,* 1993; Kaczmarczyk *et al.,* 2011; Kiełbasiński *et al.,* 2003; Ko *et al.,* 2007; Patterson & Miller, 2010; Rachwalski *et al.*, 2008; Santaniello *et al.,* 2006; Waagen *et al.,* 1993). Numerous examples pertain to the stereoselective synthesis of chiral intermediates for the production of various pharmaceuticals and plant-protecting agents (Andualema & Gessesse, 2012; Baldessari, 2012; Naik *et al.,* 2010; Sharma *et al.,* 2011; Song *et al.,* 2008). Moreover, there are many cases of promiscuous reactions catalyzed by CAL-B, including aldol reactions, Michael additions, vinyl polymerization, and even oxidations (Branneby *et al.,* 2004; Carboni-Oerlemans *et al.,* 2006; Carlqvist *et al.,* 2003; Carlqvist *et al.,* 2005; Hult & Berglund, 2007; Madalińska *et al.,* 2012; Rustoy *et al.,* 2007; Sharma *et al.,* 2009; Svedendahl *et al.,* 2005; Wu *et al.,* 2010).

Structurally, lipase B from *Candida antarctica* (CAL-B) is a macromolecule with molecular mass of about 33 kDa and 317 amino acid residues in its polypeptide chain.

✉e-mail: blaszcz8@cbmm.lodz.pl

PDB accession numbers: 4ZV7, Crystal structure of hexagonal form of lipase B from *Candida antarctica*

Abbreviations: CAL-B, Lipase B from *Candida antarctica*; NAG, N-acetyl-D-glucosamine; RMSD, Root-Mean-Square deviations; PDB, the Protein Data Bank

The active site is composed of a catalytic triad Ser-His-Asp, an oxyanion hole that stabilizes the transition state of the reaction, and a binding pocket consisting of two compartments, one for the acyl moiety of the ester and another one for the alcohol part (Otto *et al.,* 2000; Uppenberg *et al.,* 1994; Uppenberg *et al.,* 1995).

In order to improve thermostability, activity, stereoselectivity, and expression rate of CAL-B and to tailor it for different applications, a range of mutants have been developed, with main focus on kinetic resolution of chiral alcohols (Wu *et al.,* 2013; for details, see references 14-17 in that paper). For improvement of extracellular production of CAL-B enzyme in *Escherichia coli* and improvement of the enzyme stability, an anion tag has been added, and the structurally flexible residues within the active site were mutated. The X-ray crystal structures of CAL-B, with such sequence modifications, were determined (PDB entries 3W9B (Kim *et al.,* 2014), and 4K6G, 4K6H, 4K6K, 4K5Q (Xie *et al.,* 2014)). Since the truncated loop variant, cp283Δ7, showed substantial increase in the catalytic activity of the enzyme, the two crystal structures of that variant, in the apo form and with a bound inhibitor (PDB entries 3ICV and 3ICW, respectively), were determined (Qian *et al.,* 2009).

Of particular concern, in one of our ongoing research projects, is the kinetic resolution of racemic P-stereogenic alkoxy(hydroxymethyl)phenylphosphine oxides and P-stereogenic alkoxy(hydroxymethyl)phenylphosphine P-boranes *via* their enzymatic acetylation (Kwiatkowska *et al.,* 2011). Recently, we reported the results of molecular modeling of the hydrolysis reactions of acetoxymethyl(i-propoxy)-phenylphosphine oxide and its P-borane analogue, acetoxymethyl(i-propoxy)-phenylphosphine P-borane, promoted by the CAL-B enzyme (Krasiński *et al.,* 2012). These theoretical calculations suggested a hypothetical explanation of the stereochemistry of the observed hydrolysis reactions. At present, our goal is to confirm our theoretical results experimentally, by crystallization and X-ray crystal structure determination of the CAL-B enzyme in the form of a complex with the above mentioned heteroorganic ligands and their analogs.

In this work, we would like to present our first result of long-term crystallization screenings of commercially available enzyme candidates. While working on the crystallization screening of a newly purchased, crystallization grade sample of CAL-B enzyme, we discovered a new, hexagonal crystal form of this enzyme. This new form is hereby described in this paper. Due to high symmetry and good diffraction properties, the crystals of this form may by useful in obtaining complexes with various ligands.

MATERIALS AND METHODS

Protein purchase and screening. Lipase B from *Candida antarctica* (CAL-B) was purchased from *Hampton Research* (Aliso Viejo, CA, USA, Cat No. HR7-099). As declared by the manufacturer, it was a high quality, crystallization grade sample produced by submerged fermentation of a genetically modified *Aspergillus oryzae* microorganism. Prior to crystallization, the purchased sample has been subjected in our lab to final purification using size exclusion chromatography which was performed on an XK 16/60 column (Amersham Biosciences, Uppsala, Sweden) filled with Superdex 75 pg, where a mixture of 100 mM NaCl and 10 mM Tris (pH 7.3) was used as a buffer. The crystallization screening involved the use of the conditions provided by the protein manufacturer and also the use of the set of 50 unique solutions commercially available from Hampton Research Crystal Screen One (Aliso Viejo, CA, USA, Cat No. HR2-110). To our surprise, none of these conditions resulted in crystals of suitable quality. Therefore, we needed to explore new crystallization conditions.

Crystallization. Lipase B from *Candida antarctica* was crystallized using the vapour diffusion technique in hanging drops. We finally obtained two crystal forms: monoclinic and hexagonal. Both forms were obtained from different crystallization conditions. Monoclinic crystals grew from 22% (w/v) polyethylene glycol 4000, 0.05M sodium acetate (pH 3.6), 10% isopropanol with addition of 5% (w/v) n-octyl-β-D-glucoside. The monoclinic ($P2_1$) form is already known and reported in the literature as PDB entry 1TCB (Uppenberg *et al.,* 1994). The hexagonal ($P6_322$) form is new (*This work*). The hexagonal crystals have been obtained at room temperature (21°C) from 24% (w/v) polyethylene glycol 3350, 0.1M citric acid, and 0.1M sodium acetate (pH 5.5), by mixing equal volumes of protein (10 mg/ml protein in ultrapure water) and well solutions. The crystals appeared after 14 days and grew within a few additional days.

Data collection and processing. X-ray diffraction data for Lipase B from *Candida antarctica* were collected at 100 K using a SuperNova diffractometer (Agilent Technologies) equipped with a microfocus CuKα (1.54 Å) radiation source (0.8 mA and 50 kV) and a 160 mm Titan CCD detector. A solution, consisting of 50% polyethylene glycol 400 mixed with the reservoir solution (in a 1:1 ratio), was used as the cryoprotectant. Before cryocooling, the crystal was transferred into the cryoprotectant solution for a few seconds. The data were processed using CrysAlis^{Pro} (Agilent Technologies) and merged using Aimless program of the CCP4 package (Evans & Murshudov, 2013; Winn et al., 2011). Diffraction data were processed up to 2.0 Å resolution. The crystal is hexagonal, space group $P6_322$, and the unit cell parameters are: $a=b=89.03$ Å, and $c=137.26$ Å. Data collection and refinement statistics are summarized in Table 1.

Structure solution and refinement. The crystal structure of the hexagonal form of Lipase B from *Candida antarctica* was solved by the molecular replacement method using Phaser (McCoy, 2007; Winn *et al.,* 2011). The CAL-B structure (PDB 3W9B) (Kim *et al.,* 2014) has been used as the starting model. The model was rebuilt using Fourier maps calculated by *Coot* (Emsley *et al.,* 2010) and refined using *REFMAC5* (Murshudov *et al.,* 2011). Data collection and refinement statistics are summarized in Table 1. The electron density along the entire protein chain was well defined, and allowed to determine the position of all 317 residues of the entire protein sequence without any ambiguity. Water molecules and alternative conformers for some residues were added manually. Average B-factors were calculated using B-AVERAGE (Murshudov *et al.,* 2011). The structure was validated (Laskowski *et al.,*1993) and deposited in the Protein Data Bank as entry 4ZV7.

RESULTS AND DISCUSSION

New crystal form of the CAL-B lipase

While working with crystallization screening of a newly purchased (from Hampton Research Corp., Aliso Viejo, CA, USA) crystallization grade sample of lipase B from *Candida antarctica* (CAL-B), we discovered a new

Table 1. Data collection and refinement statistics for the hexagonal form of Lipase B from *Candida antarctica*.

PDB ID	4ZV7
Crystal system	Hexagonal
Space group	$P6_322$
Unit cell constants *a,b,c* (Å)	89.03, 89.03, 137.26
No. of molecules in asymmetric unit	1
Solvent content (%)	48.2
X-ray data collection	
Wavelength (Å)	1.54
Temperature (K)	100
Resolution range (Å)	77.11–2.00
Completeness (overall/last shell, %)	98.1/91.1
Redundancy (overall/last shell)	8.8/2.9
I/sigma (overall/last shell)	24.6/3.3
Unique reflections (overall/last shell)	22034/2534
R (merge) (overall/last shell)	0.093/0.261[1]
Refinement	
R (work)	0.144[2]
R (free)	0.193[2]
No. of protein atoms	2324
No. of NAG atoms	28
Bond lengths RMSD (Å)	0.02
Bond angles RMSD (°)	2.0
Average B, entire chain (Å^2)	23.8
Average B, main chain (Å^2)	21.3
Average B, NAG moiety (Å^2)	46.8
Ramachandran plot statistics:	
favoured regions (%)	97.0
allowed regions (%)	3.0
outliers (%)	0.0

[1]$R(merge)= \Sigma_h\Sigma_j | I_{hj} - \langle I_h \rangle | / \Sigma_h\Sigma_j I_{hj}$, where I_{hj} is the intensity of observation j of reflection h. [2]$R(work)= \Sigma_h | | F_o| - | F_c| | / \Sigma_h | F_o|$ for all reflections, where F_o and F_c are observed and calculated structure factors, respectively. R_{free} is calculated analogously for the test reflections, randomly selected and excluded from the refinement.

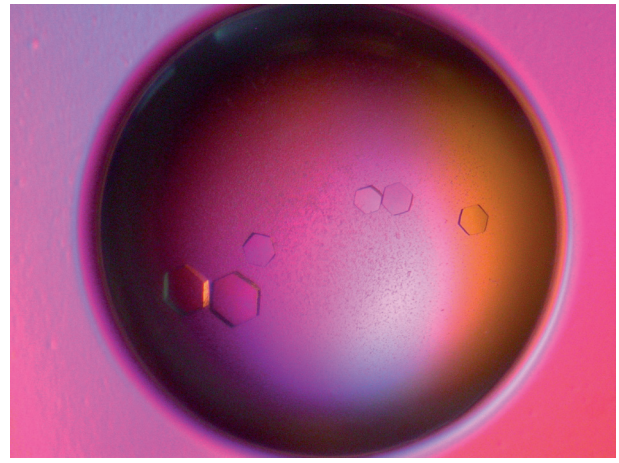

Figure 1. The crystals of the newly obtained hexagonal form of CAL-B.

crystal form of this enzyme. This new form is hereby described in this paper. The crystals of this new form are shown in Fig. 1.

The structures of lipase CAL-B, which have been reported in literature and are available in the Protein Data Bank (PDB) to date, are listed in Table 2. As is seen in Table 2, only structures 1TCA, 1TCB and 1TCC (*Uppenberg et al.*, 1994) are directly related to our newly obtained hexagonal form, 4ZV7. All four structures are of the wild-type enzyme and do not contain a ligand in the active center. Therefore, the further structural comparison and discussion will be limited to these four (4ZV7, 1TCA, 1TCB and 1TCC) structures.

Description of the hexagonal crystal form of CAL-B

The new crystal form of CAL-B (4ZV7) is hexagonal, and the space group is $P6_322$ (see Table 1). A single protein monomer is present in the asymmetric unit. The structure contains all 317 residues of the protein sequence, two NAG (N-acetyl-D-glucosamine) molecules, and 331 water molecules. All protein residues are very well visible in electron density, without any ambiguity. Four residues: Ser28, Thr159, Arg242 and Arg309, have two different conformations of their side-chains. There are two cis-peptide bonds present in the structure: one between Pro69 and Pro70 and the second between Gln191 and Pro192. The conformation of the molecule is stabilized by the presence of three disulfide bridges: Cys22-Cys64, Cys216-Cys258, and Cys293-Cys311. The presence and connectivity of these disulfide bridges, align well with those structural elements present in the orthorhombic and monoclinic forms (PDB entries 1TCA and 1TCB) (Uppenberg *et al.,* 1994).

Orthorhombic *versus* hexagonal form: similarities and differences

Both orthorhombic and hexagonal forms crystallize with the presence of single protein monomers in the respective asymmetric units. The fold of the CAL-B molecule in the hexagonal form resembles well the fold in the orthorhombic form 1TCA, with identical connectivities of the central β-sheet, and the same, right-handed, β-α-β structural motif (Uppenberg *et al.,* 1994). The entire Cα backbones of hexagonal (4ZV7) and orthorhombic (1TCA) forms align with the RMSD value of only 0.66 Å.

Table 2. The crystal structures of CAL-B lipase determined to date.

PDB code	Crystal system	Space group	Number of molecules in asymmetric unit	Number of residues in single chain	Resolution (Å)	Ligand present in active site	Reference
4ZV7	Hexagonal	$P6_322$	1	317[a]	2.00	apo form	(This work)
1TCA	Orthorhombic	$P2_12_12_1$	1	317[a]	1.55	apo form	(Uppenberg *et al.,* 1994)
1TCB	Monoclinic	$P2_1$	2	317[a]	2.10	apo form	(Uppenberg *et al.,* 1994)
1TCC	Monoclinic	$P2_1$	2	317[a]	2.50	apo form	(Uppenberg *et al.,* 1994)
1LBS	Monoclinic	C2	6	317[a]	2.60	HEE[e]	(Uppenberg *et al.,* 1995)
1LBT	Monoclinic	$P2_1$	2	317[a]	2.50	T80[f]	(Uppenberg *et al.,* 1995)
3ICV	Trigonal	$P3_221$	1	316[b]	1.49	BTB[g]	(Qian *et al.,* 2009)
3ICW	Trigonal	$P3_221$	1	316[b]	1.69	MHH[h]	(Qian *et al.,* 2009)
3W9B	Hexagonal	$P6_5$	4	328[c]	2.90	apo form	(Kim *et al.,* 2014)
4K5Q	Orthorhombic	$C222_1$	1	325[d]	1.49	apo form	(Xie *et al.,* 2014)
4K6H	Monoclinic	$P2_1$	2	326[d]	1.60	apo form	(Xie *et al.,* 2014)
4K6K	Orthorhombic	$P2_12_12_1$	2	326[d]	1.60	apo form	(Xie *et al.,* 2014)
4K6G	Monoclinic	$P2_1$	2	327[c]	1.50	apo form	(Xie *et al.,* 2014)

[a]wild-type form; [b]deletion mutant; [c]sequence variant with anion tag; [d]sequence variant with anion tag and mutations; [e]HEE, the abbreviation for N-hexylphosphonate ethyl ester in Protein Data Bank Ligand Database; [f]T80, methylpenta(oxyethyl) heptadecanoate; [g]BTB, 2[bis-(2-hydroxy-ethyl)-amino]2-hydroxymethyl-propane-1,3-diol; [h]MHH, hexyl-methoxy-phosphinic acid

The number of multiple conformations of the side chains is different in both forms. In the orthorhombic form (1TCA) the side chains, for which two conformations were found, are: Ser26, Ile87, and Leu144 (Uppenberg *et al.,* 1994).

The hexagonal form of CAL-B was crystallized in the absence of any (in particular heteroorganic) ligands. The active center of the enzyme, which involves the presence of the catalytic triad residues, Ser105, Asp187, and His224, is open, and only water molecules (eight waters: 906, 961, 1089, 1178, 1200, 1211, 1218, 1230) are found tightly buried there. Therefore, our hexagonal structure is a ligand-free (apo) form of the enzyme (see Table 2).

Interestingly, there are more water molecules in the active center in our hexagonal structure than in the orthorhombic form, where only four water molecules were found (Uppenberg *et al.,* 1994). The catalytic triad residues Ser105, Asp187, and His224, in the active site in the orthorhombic form, 1TCA, have almost identical position and conformation, except for the Cβ-Oγ bond of Ser105, which rotates slightly away from the $N\varepsilon_2$ atom of His224. The movement of the Oγ atom of Ser105 is about 0.5 Å.

The protein side chains in the hexagonal form of the enzyme are thermally quite stable. The difference between average mobilities of the entire chain (B=23.8 Å^2) and of the main chain atoms (B=21.3 Å^2) is very small (Table 1). Interestingly, in contrast to the orthorhombic form, where the increased mobility was observed for the side chains of the catalytic triad residues Ser105-Asp187-His224, and where this phenomenon has been suggested to be of functional interest (Uppenberg *et al.,* 1994), our hexagonal form does not show any sign of such mobility increase.

Unexpected opening of the glycosylation site in hexagonal CAL-B. Is this opening functionally related?

In both orthorhombic (1TCA) and hexagonal (4ZV7) forms, the NAG molecules are present in the glycosylation site and bound to the side chain $N\delta_2$ atom of the Asn74 residue (Fig. 2). However, the positions of these NAG molecules do not align with each other (Fig. 3). In the hexagonal form, the side chain of Asn74 and two visible bound NAG molecules rotate straight out of the protein molecule towards the solvent region. In the orthorhombic form, this side chain and two NAG

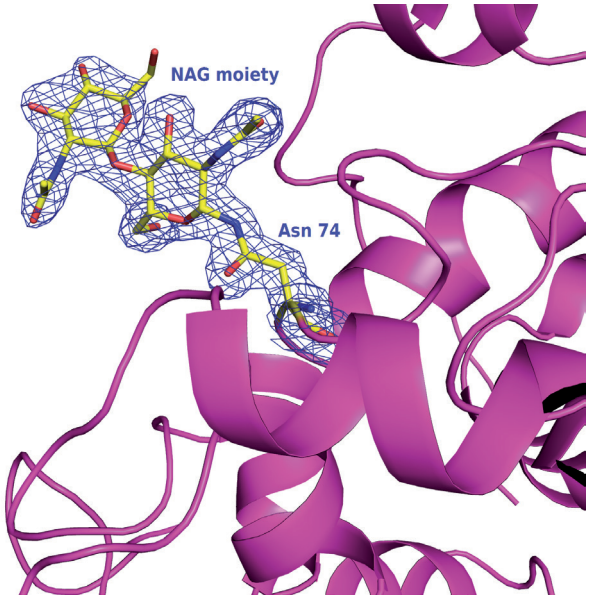

Figure 2. View of the glycosylation site, and the omit map for the NAG moiety and residue Asn74, in the hexagonal form of CAL-B.
The NAG moiety, and residue Asn74 to which it is bound, are shown as stick models in the atomic color scheme (nitrogen in blue and oxygen in red). The electron density for these elements is shown as a blue net.

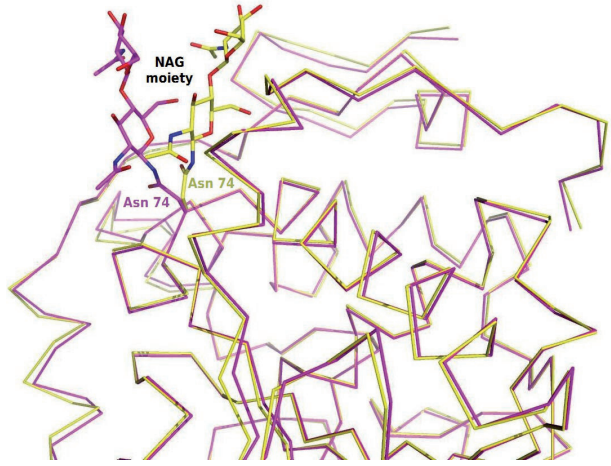

Figure 3. Alignment of the Cα backbones near the glycosylation sites of the orthorhombic (1TCA, in yellow) and the hexagonal (4ZV7, in magenta) forms of CAL-B.
The alignment reveals opening (4ZV7) and closing (1TCA) of the glycosylation site, by the 'lid' NAG moiety, bound to the side chain $N\delta_2$ atom of Asn74 residue.

molecules rotate towards the enzyme molecule, and close the glycosylation site (Fig. 3). The torsion angle N-Cα-Cβ-Cγ of Asn74, which describes this rotation, in the orthorhombic form is –163°, but in the hexagonal form this angle is –96°, and resulting in a difference of about 70 degrees.

There are significant differences in interactions, between NAG moiety and the protein, in both forms. In orthorhombic form (1TCA), the first NAG molecule in the chain (the one bound to Asn74) has an extended system of contacts with the protein. There are two direct contacts to the side chains: (NAG1) O3 — 3.22 Å — (Gln11) NE2; and (NAG1) O6 — 2.75 Å — (Asp75) OD2. Additionally, four contacts of NAG1 are to protein side chains *via* water molecules: (NAG1) O6 — 2.69 Å — (Wat515) — 2.96 Å — (Ser10) OG; (NAG1) O7 — 2.64 Å — (Wat436) — 2.82 Å — (Gln11) OE1; (NAG1) O7 — 2.64 Å — (Wat436) — 2.76 Å — (Tyr82) OH and (NAG1) O7 — 2.74 Å — (Wat567) — 3.25 Å — (Asn79) OD1. The side chain of Asn74, to which the NAG chain is bound, also has one water molecule involved: (Asn74) OD1 — 2.84 Å — (Wat492). The second NAG molecule in the chain is not involved in any intramolecular contacts with the protein in the orthorhombic form. It is involved only in intermolecular contacts, mainly with solvent molecules. The shortest intermolecular distance of NAG2 to the protein side chain of symmetry-related molecule is: (NAG2) O7 — 4.23 Å — (Arg238) NH1. In the hexagonal form (4ZV7), the contacts of NAG1 molecule are: (NAG1) O6 — 2.77 Å — (Wat1015) — 2.85 Å — (Wat953) — 2.63 Å — (Asp75) OD2; (NAG1) O7 — 2.65 Å — (Wat958) — 2.56 Å — (Wat1102) and (NAG1) O7 — 2.65 Å — (Wat958) — 2.79 Å — (Wat907) — 2.39 Å — (Tyr82) OH. The Asn74 residue, to which the NAG chain is bound, has similarly a contact with water molecule: (Asn74) OD1 — 2.81 Å — (Wat1038), but this water is located in different place, i.e., does not superimpose with respective water from orthorhombic structure. More, the side chain of residue Asp75, which is next to Asn74, in hexagonal form has its side chain rotated out of the NAG chain. The respective average B-factors for NAG2 and NAG1 are 61.9 $Å^2$ and 31.6 $Å^2$. Similar mobility difference between the first and the second NAG molecule in the chain has been observed in the orthorhombic form.

The electron density for the NAG moiety is well defined and highly comparable to the density of the side chain of residue Asn74, to which the NAG moiety is bound (Fig. 2). In the hexagonal form, the entire NAG moiety has increased mobility, in comparison with the protein chain. For example, the avarage value of the B-factor for the NAG moiety is 46.8 $Å^2$ (see Table 1), whereas the average B-factor for residue Asn74 is 19.7 $Å^2$. Similar mobility increase was observed for the NAG moiety in the orthorhombic form, where the average B-factor values were 27.7 $Å^2$ and 8.7 $Å^2$, for the NAG moiety and residue Asn74, respectively.

Such a significant opening of the glycosylation site in the hexagonal form, when compared to a partial closing of this site in the orthorhombic form, is probably the reason that the two regions: first, which involves residues 266–287, and second, which involves C-terminal residues 306–317, do not superimpose well.

We do not know whether the opening (in the hexagonal form) and closing (in the orthorhombic form) of the glycosylation site, by the 'lid' NAG molecules, is just an effect of the crystal packing, or it could be related to the opening and closing of the enzyme active center upon substrate binding and product release.

Conserved, tightly buried water, in all crystal forms

Of special interest (Uppenberg *et al.,* 1994) is the water molecule (Water number 950 in hexagonal form) which is bound to the $O\delta_2$ atom of the active site residue Asp187 (distance 2.63 Å in hexagonal form) and to the Oγ atom of Ser227 residue (distance 3.12 Å in hexagonal form). This water, in the orthorhombic form 1TCA, is located in the same place and has the same

connection system. While the distance of this water to Asp187 is similar (2.67 Å), the connection with Ser227 in the orthorhombic form is much tighter (2.87 Å). The connectivity of this water molecule in the monoclinic form 1TCB resembles well the situation in the orthorhombic structure. The respective distances of this water are: 2.88 Å (to Asp187) and 2.80 Å (to Ser227) in monomer 1TCB-A, and, respectively, 2.72 Å and 3.01 Å, in monomer 1TCB-B.

Structural comparison of hexagonal, orthorhombic and monoclinic forms

The protein molecule of the orthorhombic form (1TCA) alignes very well with the two independent protein molecules A and B of the monoclinic form (1TCB), including not only a good alignment of Cα backbones, but also the alignment of the two NAG molecules that are visible in the glycosylation site of molecule A of the monoclinic form (Uppenberg *et al.,* 1994). The RMSD value of alignment of 1TCA to 1TCB-A is 0.53 Å, and the RMSD value of alignment of 1TCA to 1TCB-B is 0.52 Å. The RMSD values, for alignment of 4ZV7 to 1TCB-A, and for alignment of 4ZV7 to 1TCB-B, are both equal to 0.64 Å.

Since the orthorhombic (1TCA) and monoclinic (1TCB) forms align well, the differences, which were discussed for the Cα backbone conformation and the position of the NAG molecules bound to the side chain of Asn74 in the hexagonal (4ZV7) and the orthorhombic (1TCA) forms, apply to the same extent to the comparison of the hexagonal form (4ZV7) with the monoclinic form (1TCB) (Uppenberg *et al.,* 1994).

The striking difference between the three crystal forms: monoclinic (1TCB and 1TCC), orthorhombic (1TCA) and hexagonal (4ZV7), is obviously the packing of the protein molecules in the crystals, and the number of molecules that are present in the asymmetric units. In monoclinic forms 1TCB and 1TCC, the two molecules are present in the asymmetric units. These two independent monomers, 1TCB-A and 1TCB-B, are packed in such way that the large hydrophobic surface around the active site pocket of one molecule packs against the corresponding surface of the other molecule (Uppenberg *et al.,* 1994). In orthorhombic form (1TCA), where a single monomer is present in the asymmetric unit, the hydrophobic surface is packed against a neighboring molecule, with the side chain of Leu199 from a symmetry-related molecule pointing into the active center and therefore partly responsible for stabilization of the opening of active site channel.

In the hexagonal form (4ZV7), where also a single monomer is present in the asymmetric unit, the active site of a monomer is packed towards the active site of a symmetry-related molecule. Such packing of the symmetrical pairs extends along the crystallographic *c*-axis.There is no sign of any dimerization between these pairs. Instead, the active sites which point towards each other in the symmetrical neighbors, create a solvent-accessible channel, which extends along the entire planes, which are parallel to the plane formed by the unit-cell edges *a* and *b*. Such packing of all molecules in the crystal makes the active centers very well accessible for the ligands.

Acknowledgements

Financial support by the Polish National Science Center, grant No. DEC-2012/05/B/ST4/00075, is gratefully acknowledged. The authors used BL14.1 beamline operated by the Helmholtz-Zentrum Berlin (HZB) at the BESSY II electron storage ring (Berlin-Adlershof, Germany) for diffraction tests and collection of the initial data sets from the lipase microcrystals. The coordinates and structure factors of the hexagonal form of CAL-B apoenzyme have been deposited in the Protein Data Bank (PDB), as entry 4ZV7.

REFERENCES

Alatorre-Santamaria S, Gotor-Fernandez V, Gotor V (2011) Chemoenzymatic synthesis of optically active cis- and trans-2-(1H-imidazol-1-yl)cycloalkanamines. *Eur J Org Chem* **6**: 1057–1063. doi: 10.1002/ejoc.201001299.

Andualema B, Gessesse A (2012) Microbial lipases and their industrial applications: review. *Biotechnology* **11**: 100–118. doi: 10.3923/biotech.2012.100.118.

Bornscheuer UT, Kazlauskas RJ (1999) *Hydrolases in organic synthesis: regio- and stereoselective biotransformations*. Wiley-VCH, Weinheim, Germany. doi: 10.1002/3527607544.ch7.

Branneby C, Carlqvist P, Hult K, Brinck T, Berglund P (2004) Aldol additions with mutant lipase: analysis by experiments and theoretical calculations. *J Mol Catal B Enzym* **31**: 123–128. doi: 10.1016/j.molcatb.2004.08.005.

Baldessari A (2012) Lipases as catalysts in synthesis of fine chemicals. *Meth Mol Biol* **861**: 445–456. doi: 10.1007/978-1-61779-600-5_25.

Carboni-Oerlemans C, Dominguez de Maria P, Tuin B, Bargeman G, van der Meer A, van Gemert R (2006) Hydrolase-catalysed synthesis of peroxycarboxylic acids: biocatalytic promiscuity for practical applications. *J Biotechnol* **126**: 140–151. doi:10.1016/j.jbiotec.2006.04.008.

Carlqvist P, Eklund R, Hult K, Brinck T (2003) Rational design of a lipase to accommodate catalysis of Baeyer-Villiger oxidation with hydrogen peroxide. *J Mol Model* **9**: 164–171. DOI 10.1007/s00894-003-0128-y.

Carlqvist P, Svedendahl M, Branneby C, Hult K, Brinck T, Berglund P (2005) Exploring the active-site of a rationally redesigned lipase for catalysis of Michael-type additions. *ChemBioChem* **6**: 331–336. doi: 10.1002/cbic.200400213.

Colton IJ, Yin DL, Grochulski P, Kazlauskas RJ (2011) Molecular basis of chiral acid recognition by *Candida rugosa* lipase: X-ray structure of transition state analog and modeling of the hydrolysis of methyl 2-methoxy-2-phenylacetate. *Adv Synth Catal* **353**: 2529–2544. doi: 10.1002/adsc.201100459.

Cygler M, Grochulski P, Kazlauskas RJ, Schrag JD, Bouthillier F, Rubin B, Serreqi AN, Gupta AK (1994) A structural basis for the chiral preferences of lipases. *J Am Chem Soc* **116**: 3180–3186. doi: 10.1021/ja00087a002.

Deska J, Ochoa CD, Backvall JE (2010) Chemoenzymatic dynamic kinetic resolution of axially chiral allenes. *Chem Eur J* **16**: 4447–4451. doi: 10.1002/chem.201000301.

Emsley P, Lohkamp B, Scott WG, Cowtan K (2010) Features and development of Coot. *Acta Cryst* **D66**: 486–501. doi: 10.1107/S0907444910007493.

Evans PR, Murshudov GN (2013) How good are my data and what is the resolution? *Acta Cryst* **D69**: 1204–1214. doi:10.1107/S0907444913000061.

Frykman H, Ohrner N, Norin T, Hult K (1993) S-Ethyl thiooctanoate as acyl donor in lipase-catalyzed resolution of secondary alcohols. *Tetrahedron Lett* **34**: 1367–1370. doi: 10.1016/S0040-4039(00)91797-0.

Grochulski P, Li Y, Schrag JD, Bouthillier F, Smith P, Harrison D, Rubin B, Cygler M (1993) Insights into interfacial activation from an open structure of *Candida rugosa* lipase. *J Biol Chem* **268**: 12843–12847. PMID: 8509417.

Grochulski P, Bouthillier F, Kazlauskas RJ, Serreqi AN, Schrag JD, Ziomek E, Cygler M (1994) Analogs of reaction intermediates identify a unique substrate binding site in *Candida rugosa* lipase. *Biochemistry* **33**: 3494–3500. doi: 10.1021/bi00178a005.

Grochulski P, Li Y, Schrag JD, Cygler M (1994) Two conformational states of *Candida rugosa* lipase. *Protein Sci* **3**: 82–91. doi: 10.1002/pro.5560030111.

Hult K, Berglund P (2007) Enzyme promiscuity: mechanism and applications. *Trends Biotechnol* **25**: 231–238. doi: 10.1016/j.tibtech.2007.03.002.

Kaczmarczyk S, Kwiatkowska M, Madalińska L, Barbachowska A, Rachwalski M, Błaszczyk J, Sieroń L, Kielbasiński P (2011) Enzymatic synthesis of enantiopure precursors of chiral bidentate and tridentate phosphorus catalysts. *Adv Synth Catal* **353**: 2446–2454. doi: 10.1002/adsc.201100280.

Kiełbasiński P, Żurawiński R, Albrycht M, Mikołajczyk M (2003) The first enzymatic desymmetrizations of prochiral phosphine oxides. *Tetrahedron Asymmetry* **14**: 3379–3384. doi: 10.1016/j.tetasy.2003.08.003.

Kiełbasiński P, Mikołajczyk M (2007) Chiral heteroatom-containing compounds. In *Future directions in biocatalysis*. Matsuda T, ed, pp 159–203. Elsevier. doi: 10.1016/B978-044453059-2/50009-1.

Kim KK, Song HK, Shin DH, Hwang KY, Suh SW (1997) The crystal structure of a triacylglycerol lipase from *Pseudomonas cepacia* reveals a highly open conformation in the absence of a bound inhibitor. *Structure* **5**: 173–185. doi: 10.1016/S0969-2126(97)00177-9.

Kim SK, Lee HH, Park YC, Jeon ST, Son SH, Min WK, Seo JH (2014) Crystal structure of *Candida antarctica* lipase B with anion-tag. *The Protein Data Bank (PDB) entry 3W9B*. doi: 10.2210/pdb3w9b/pdb.

Kirk O, Christensen MW (2002) Lipases from *Candida antarctica*: unique biocatalysts from a unique origin. *Org Prog Res Dev* **6**: 446–451. doi: 10.1021/op0200165.

Ko SB, Baburaj B, Kim MJ, Park J (2007) Air-stable racemization catalysts for the dynamic kinetic resolution of secondary alcohols. *J Org Chem* **72**: 6860–6864. doi: 10.1021/jo071065o.

Krasiński G, Cypryk M, Kwiatkowska M, Mikołajczyk M, Kiełbasiński P (2012) Molecular modeling of the lipase-catalyzed hydrolysis of acetoxymethyl(ı-propoxy) phenylphosphine oxide and its P-borane analogue. *J Mol Graph Model* **38**: 290–297. doi: 10.1016/j.jmgm.2012.09.001.

Kwiatkowska M, Krasiński G, Cypryk M, Cierpiał T, Kiełbasiński P (2011) Lipase-mediated stereoselective transformations of chiral organophosphorus P-boranes revisited: revision of the absolute configuration of alkoxy(hydroxymethyl)phenylphosphine P-boranes. *Tetrahedron Asymmetry* **22**: 1581–1590. doi: 10.1016/j.tetasy.2011.08.024.

Madalińska L, Kwiatkowska M, Cierpiał T, Kiełbasiński P (2012) Investigations on enzyme catalytic promiscuity: the first attempts at a hydrolytic enzyme-promoted conjugate addition of nucleophiles to α,β-unsaturated sulfinyl acceptors. *J Mol Catal B Enzym* **81**: 25–30. doi: 10.1016/j.molcatb.2012.05.002.

Mancheno JM, Pernas MA, Martinez MJ, Ochoa B, Rua ML, Hermoso JA (2003) Structural insights into the lipase/esterase behavior in the *Candida rugosa* lipases family: crystal structure of the lipase 2 isoenzyme at 1.97 Å resolution. *J Mol Biol* **332**: 1059–1069. doi: 10.1016/j.jmb.2003.08.005.

McCoy AJ (2007) Solving structures of protein complexes by molecular replacement with Phaser. *Acta Cryst* **D63**: 32–41. doi:10.1107/S0907444906045975.

Murshudov GN, Skubak P, Lebedev AA, Pannu NS, Steiner RA, Nicholls RA, Winn MD, Long F, Vagin AA (2011) REFMAC5 for the refinement of macromolecular crystal structures. *Acta Cryst* **D67**: 355–367. doi: 10.1107/S0907444911001314.

Naik S, Basu A, Saikia R, Madan B, Paul P, Chaterjee R, Brask J, Svendsen A (2010) Lipases for use in industrial biocatalysis: specificity of selected structural groups of lipases. *J Mol Catal B Enzym* **65**: 18–23. doi: 10.1016/j.molcatb.2010.01.002.

Otto RT, Scheib H, Bornscheuer UT, Pleiss J, Syldatk C, Schmid RD (2000) Substrate specificity of lipase B from *Candida antarctica* in the synthesis of aryl aliphatic glycolipids. *J Mol Catal B Enzym* **8**: 201–211. doi: 10.1016/S1381-1177(99)00058-2.

Paravidino M, Groger H, Hanefeld U (2012) In *Enzyme Catalysis in. Organic Synthesis*. Drauz K, Groger H, May O, eds, pp 251–362. Wiley-VCH, Weinheim, Germany. doi: 10.1002/9783527639861.ch8.

Patterson LD, Miller MJ (2010) Enzymatic deprotection of the cephalosporin 3'-acetoxy group using *Candida antarctica* lipase B. *J Org Chem* **75**: 1289–1292. doi: 10.1021/jo902406b.

Qian Z, Horton JR, Cheng X, Lutz S (2009) Structural redesign of lipase B from *Candida antarctica* by circular permutation and incremental truncation. *J Mol Biol* **393**: 191–201. doi: 10.1016/j.jmb.2009.08.008.

Rachwalski M, Kwiatkowska M, Drabowicz J, Kłos M, Wieczorek WM, Szyrej M, Sieroń L, Kiełbasiński P (2008) Enzyme-promoted desymmetrization of bis(2-hydroxymethylphenyl) sulfoxide as a route to tridentate chiral catalysts. *Tetrahedron Asymmetry* **19**: 2096–2101. doi: 10.1016/j.tetasy.2008.08.017.

Rustoy EM, Sato Y, Nonami H, Erra-Balsells R, Baldessari A (2007) Lipase-catalyzed synthesis and characterization of copolymers from ethyl acrylate as the only monomer starting material. *Polymer* **48**: 1517–1525. doi: 10.1016/j.polymer.2007.01.040.

Santaniello E, Casati S, Ciuffreda P (2006) Lipase-catalyzed deacylation by alcoholysis: a selective, useful transesterification reaction. *Curr Org Chem* **10**: 1095–1123. doi: 10.2174/138527206777698110.

Sharma D, Sharma B, Shukla AK (2011) Biotechnological approach of microbial lipase: a review. *Biotechnology* **10**: 23–40. doi: 10.3923/biotech.2011.23.40.

Sharma UK, Sharma N, Kumar R, Kumar R, Sinha AK (2009) Biocatalytic promiscuity of lipase in chemoselective oxidation of aryl alcohols/acetates: a anique synergism of CAL-B and Br for the metal-free H_2O_2 activation. *Org Lett* **11**: 4846–4848. doi: 10.1021/ol901917e.

Singh AK, Mukhopadhyay M (2012) Overview of fungal lipase: A review. *Appl Biochem Biotechnol* **166**: 486–520. doi: 10.1007/s12010-011-9444-3.

Song X, Qi X, Hao B, Qu Y (2008) Studies of substrate specificities of lipases from different sources. *Eur J Lipid Sci Technol* **110**: 1095–1101. doi: 10.1002/ejlt.200800073.

Svedendahl M, Hult K, Berglund P (2005) Fast carbon-carbon bond formation by a promiscuous lipase. *J Am Chem Soc* **127**: 17988–17989. doi: 10.1021/ja056660r.

Uppenberg J, Hansen MT, Patkar S, Jones TA (1994) The sequence, crystal structure determination and refinement of two crystal forms of lipase B from *Candida antarctica*. *Structure* **2**: 293–308. doi:10.1016/S0969-2126(00)00031-9.

Uppenberg J, OehrnerN, Norin M, Hult K, Kleywegt GJ, Patkar S, Waagen V, Anthonsen T, Jones TA (1995) Crystallographic and molecular-modeling studies of lipase B from *Candida antarctica* reveal a stereospecificity pocket for secondary alcohols. *Biochemistry* **34**: 16838–16851. doi: 10.1021/bi00051a035.

Waagen V, Hollingstaeter I, Partali V, Thorstad O, Anthonsen T (1993) Enzymatic resolution of butanoic esters of 1-phenyl, 1-phenylmethyl, 1-[2-phenylethyl] and 1-[2-phenoxyethyl]ethers of 3-methoxy-1,2-propanediol. *Tetrahedron Asymmetry* **4**: 2265–2274. doi: 10.1016/S0957-4166(00)80077-4.

Winn MD, Ballard CC, Cowtan KD, Dodson EJ, Emsley P, Evans PR, Keegan RM, Krissinel EB, Leslie AGW, McCoy A, McNicholas SJ, Murshudov GN, Pannu NS, Potterton EA, Powell HR, Read RJ, Vagin A, Wilson KS (2011) Overview of the CCP4 suite and current developments. *Acta Cryst* **D67**: 235–242. doi: 10.1107/S0907444910045749.

Wu Q, Liu BK, Lin XF (2010) Enzymatic promiscuity for organic synthesis and cascade process. *Curr Org Chem* **14**: 1966–1988. doi: 10.2174/138527210792927591.

Wu Q, Soni P, Reetz MT (2013) Laboratory evolution of enantiocomplementary *Candida antarctica* lipase B mutants with broad substrate scope. *J Am Chem Soc* **135**: 1872–1881. doi: 10.1021/ja310455t.

Xie Y, An J, Yang G, Wu G, Zhang Y, Cui L, Feng Y (2014) Enhanced enzyme kinetic stability by increasing rigidity within the active site. *J Biol Chem* **289**: 7994–8006. doi: 10.1074/jbc.M113.536045.